JOURNAL OF AIRCRAFT
Vol. 29, No. 5, Sept.–Oct. 1992

Engineering Notes

ENGINEERING NOTES are short manuscripts describing new developments or important results of a preliminary nature. These Notes cannot exceed 6 manuscript pages and 3 figures; a page of text may be substituted for a figure and vice versa. After informal review by the editors, they may be published within a few months of the date of receipt. Style requirements are the same as for regular contributions (see inside back cover).

Improved Calculation of Transonic Potential Flow Past Swept Wings

Lixia Wang* and David A. Caughey†
Cornell University, Ithaca, New York 14853

Introduction

In spite of recent advances in numerical methods to solve the Euler and Navier-Stokes equations for transonic flow problems, the transonic potential equation is still widely used in design work. Among the algorithms for solving three-dimensional transonic potential flows, the computer program Flo-22 developed by Jameson and Caughey[1] has proved to be economical and robust for many practical applications.

The purpose of this note is to describe some recent improvements in Flo-22, that include a chordwise scaling to render the trailing edge a grid line, and a modification to the symmetry plane boundary condition to better enforce the no-flux condition there. Results are presented for the transonic flow past a supercritical wing, using the original and modified versions of Flo-22, as well as the fully-conservative Euler code developed by Yadlin and Caughey.[2]

Flo-22 Program

The original program Flo-22 is designed to calculate the transonic potential flow past a wing of arbitrary planform and dihedral extending from a plane wall. A body-conforming coordinate system is generated by a sequence of elementary transformations so that the spanwise coordinate lines are aligned with the leading edge but are not parallel to the trailing edge when the wing has taper.

The nonconservative, three-dimensional transonic potential equation has the form

$$(a^2 - u^2)\Phi_{xx} + (a^2 - v^2)\Phi_{yy} + (a^2 - w^2)\Phi_{zz} - 2uv\Phi_{xy} - 2uw\Phi_{xz} - 2vw\Phi_{yz} = 0 \tag{1}$$

where Φ is the velocity potential, u, v, and w are the velocity components in the x, y, and z Cartesian coordinate directions and a is the local speed of sound. For the steady, constant energy flow of a perfect gas of specific heat ratio γ

$$a^2 = a_0^2 - \left[\frac{(\gamma - 1)}{2}\right](u^2 + v^2 + w^2)$$

where a_0 is the stagnation speed of sound.

Received July 15, 1991; revision received Sept. 15, 1991; accepted for publication Oct. 14, 1991.

*Graduate Research Assistant, Sibley School of Mechanical and Aerospace Engineering.

†Professor, Sibley School of Mechanical and Aerospace Engineering. Associate Fellow AIAA.

Since the flow is assumed uniform at infinity, the far-field singularity in the velocity potential is removed by defining the reduced potential

$$G = \Phi - x\cos\alpha - y\sin\alpha$$

where α is the angle-of-attack.

The equation for the reduced potential G, obtained by transforming Eq. (1) from the physical plane to the computational plane, is solved by a finite difference method using the rotated difference scheme of Jameson[3] in nonconservative form. The difference equations are solved by "successive line over relaxation." A complete description of the original program can be found in Ref. 1.

Recent Improvements

Chordwise Scaling

The wing trailing edge is made a grid line by introducing the chordwise scaling

$$\bar{x} = \frac{x - x_s(z)}{c(z)}$$
$$\bar{y} = \frac{y - y_s(z)}{c(z)} \tag{2}$$
$$\bar{z} = z$$

where $x_s(z)$ and $y_s(z)$ represent the location of a singular line just inside the leading edge of the profile at each spanwise station, and $c(z)$ is the distance between the trailing edge and the singular line in each spanwise plane. For the planes beyond the wing tip, $c(z)$ is artificially defined as $c(z) = c(z_{tip})$. This transformation shears out the wing sweep and dihedral, puts the singular line at the origin of each $\bar{x}$, $\bar{y}$ plane, and normalizes the coordinates in the streamwise and vertical directions. In each of these planes, parabolic coordinates are introduced by the square-root transformation

$$(X_1 + iY_1)^2 = 2(\bar{x} + i\bar{y})$$
$$Z_1 = \bar{z} \tag{3}$$

The effect of this transformation is to unwrap the wing to form a shallow bump near the plane $Y_1 = 0$. If the height of this bump is defined as

$$Y_1 = S(X_1, \bar{z})$$

then the final shearing transformation

$$X = X_1$$
$$Y = Y_1 - S(X_1, \bar{z}) \tag{4}$$
$$Z = \bar{z}$$

maps the wing surface to a portion of the coordinate surface $Y = 0$. In the resulting coordinate system, both the leading and trailing edges are lines of constant X in the surface $Y =$

0, so that the same number of mesh cells lie on the wing surface in each spanwise plane.

Since the equation for the reduced potential G is transformed from (x, y, z) to (X, Y, Z), some additional complexity is introduced by the scaling of the coordinates with the local chord $c(z)$; this requires approximately 30% more computational work per iteration for the modified version. Details of the transformed equations are given by Wang and Caughey.[4]

Symmetry Plane Modification

In the original Flo-22, the spanwise coordinate line is extended linearly through the symmetry plane, and the boundary condition that $w = 0$ is enforced on the surface $Z = 0$ by requiring

$$cG_Z + \zeta G_X - (cS_Z + \zeta S_X - \eta)G_Y = 0 \qquad (5)$$

where

$$\eta = X_{1y}x'_s - X_{1x}y'_s + c'(X_{1y}\bar{x} - X_{1x}\bar{y})$$

$$\zeta = -X_{1x}x'_s - X_{1y}y'_s + c'(-X_{1x}\bar{x} - X_{1y}\bar{y})$$

Due to the nonorthogonality of the coordinate system when the wing is swept or tapered, simple central differences used to approximate all first derivatives in Eq. (5) can become unstable. To maintain stability, an average of one-sided differences on the computational planes on either side of $Z = 0$ was used to set the values of the potential on the image plane inside $Z = 0$ in the original program, but the usual centered formulas were still used in the solution algorithm. As a result of this inconsistency, it was found that $w = 0$ is not satisfied exactly everywhere on the symmetry plane.

In the modified version, the wing geometry is assumed to be completely symmetrical about the symmetry plane and Eq. (5) reduces to

$$G_Z = 0$$

If central differences are used to define the potential values at the image points for the symmetry plane in this case, the iterative scheme fails to converge when the wing is highly swept and/or tapered. The stability of the approximation on the symmetry plane is improved by replacing the first X-differences by weighted averages of central differences on the $Z = 0$ plane and its neighbors to either side. The same approximation is used in the solution algorithm, so that the symmetry condition is satisfied exactly, and the formal accuracy remains second order. This approach has proved stable for tapered wings at sweep angles in excess of 35 deg.

Results

As in the original version of Flo-22, grid sequencing is used in the modified version of Flo-22 to speed iterative convergence. An initial calculation is performed on a coarse grid, typically containing 48 × 6 × 8 grid cells in the X, Y, and Z directions, respectively. This solution is then interpolated onto a finer grid containing twice as many mesh cells in each direction, and is used as a starting guess for an intermediate solution. The process is repeated once again to give the final

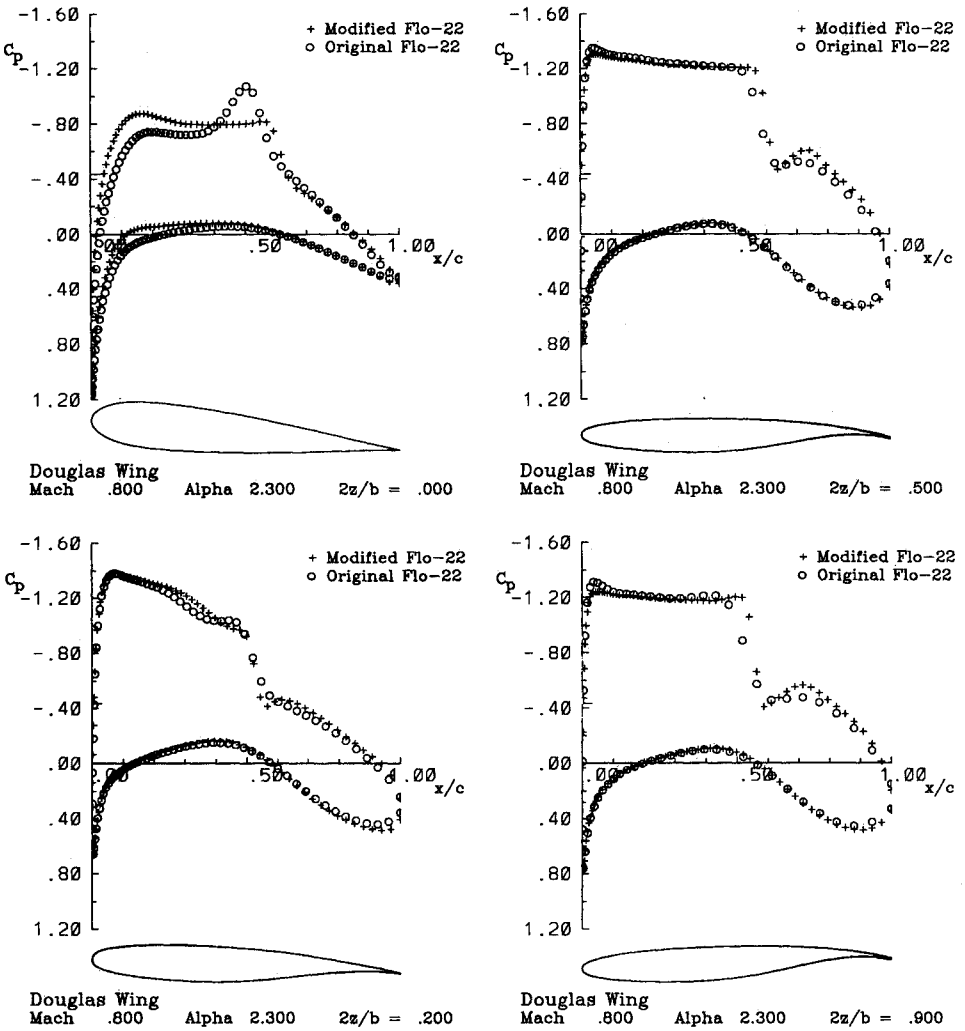

Fig. 1 Streamwise wing surface pressure distributions calculated using modified and original versions of Flo-22; flow past Douglas Wing LB-488 at freestream Mach number of 0.80- and 2.3-deg angle-of-attack.

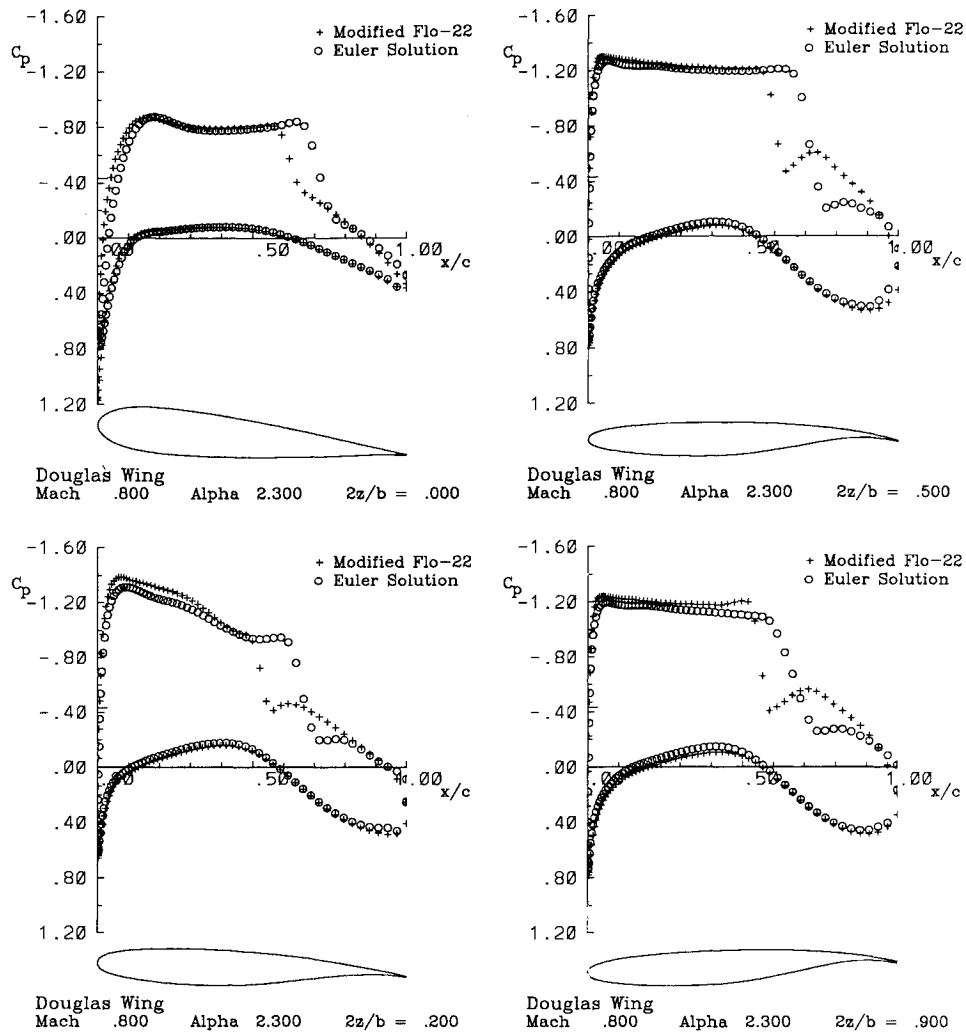

Fig. 2 Streamwise wing surface pressure distributions calculated using modified versions of Flo-22 and Euler solver; flow past Douglas Wing LB-488 at freestream Mach number of 0.80- and 2.3-deg angle-of-attack.

solution on a grid containing 192 × 24 × 32 mesh cells. Typically, 100 iterations are done on each grid level and the final solutions are quite well-converged.

All the results presented here have been computed for a typical transonic transport-type wing, here called the Douglas Wing LB-488,[5] at a Mach number of 0.80- and 2.3-deg angle-of-attack. This wing has modern supercritical wing sections, a leading-edge sweep of 33.11 deg, and a taper ratio of $c_{tip}/c_{root} = 0.2115$. The planform of this wing has a discontinuity in trailing-edge sweep at approximately 31% of the semispan.

Comparisons of the streamwise pressure distributions calculated by the modified and original versions of Flo-22 are shown in Fig. 1 at the 0, 20, 50, and 90% semispan stations, respectively. There is a noticeable difference between the two solutions at the root station, where the upper surface pressure distribution has a large spike upstream of the shock in the solution from the original Flo-22. This spike is nonphysical and is apparently introduced by the poor treatment of the symmetry plane boundary condition in the original code. In the modified version of Flo-22, the spike does not appear and the root-station pressure distribution is similar to those in neighboring computational planes. The shock positions in both calculations agree well, but the shock is more highly smeared in the original Flo-22 solution. This is due to the loss of resolution in the original version near the wing tip, where there are fewer mesh points on the wing surface at each successive spanwise section, and because the grid lines in the modified version are better aligned with the shock at the inboard stations.

In Fig. 2, the streamwise pressure distributions for the modified version of Flo-22 are also compared with those of the Euler solution of Yadlin and Caughey[2] at four spanwise stations. The three-dimensional fully-conservative Euler equations are solved using the implicit, diagonalized "alternating direction implicit" multigrid method on a mesh having the same number of grid cells and the same distribution of grid points on the wing surface as for the potential calculations. Both solutions are in good agreement except for the shock strengths and positions, particularly near the wing tip where the shock is the strongest. The shock position in the potential solution is slightly forward of the Euler solution, and the shocks are also weaker in the nonconservative potential solution. This difference is almost certainly due to the differences in the shock polars of the two models. The forward shift in location and weakening of the shock wave is consistent with the differences one would expect from a nonconservative formulation.

Conclusions

An improved version of Flo-22 for calculating the transonic potential flow past swept wings has been described. The new chordwise scaling and improved symmetry plane treatment result in a truly boundary conforming coordinate system for three-dimensional wings and consistent treatment of the no-flux condition on the symmetry plane. Results show that improvements have been made in the accuracy of the solution near the wing tip and the wing root.

Acknowledgments

This research was supported in part by the Douglas Aircraft Company of the McDonnell Douglas Corporation under Contract AS-25260-C.

References

[1]Jameson, A., and Caughey, D. A., "Numerical Calculation of the Transonic Flow Past a Swept Wing," New York Univ. ERDA Rept. COO-3077-140, New York, June 1977.

[2]Yadlin, Y., and Caughey, D. A., "Diagonal Implicit Multigrid Solution of the Three-Dimensional Euler Equations," *Proceedings of the Eleventh International Conference on Numerical Methods for Fluid Dynamics*, Vol. 323, Lecture Notes in Physics, Springer-Verlag, Berlin, June 1988, pp. 597–601.

[3]Jameson, A., "Iterative Solution of Transonic Flows over Airfoils and Wings, Including Flows at Mach 1," *Communications on Pure and Applied Mathematics*, Vol. 27, 1974, pp. 283–309.

[4]Wang, L., and Caughey, D. A., "Numerical Calculation of the Transonic Potential Flow Past a Swept Wing—An Improved Version of Program Flo-22," Cornell Univ., Sibley School of Mechanical and Aerospace Engineering, Fluid Dynamics and Aerodynamics Rept. FDA 88-17, Ithaca, NY, Aug. 1988.

[5]Steckel, D. K., Dahlin, J. A., and Henne, P. A., "Results of Design Studies and Wind Tunnel Tests of High Aspect Ratio Supercritical Wings for an Energy Efficient Transport," NASA CR-159332, 1980.

Predicting Droplet Impingement on Yawed Wings

Michael B. Bragg*
University of Illinois at Urbana—Champaign, Urbana, Illinois 61821
and
Stanley H. Mohler Jr.†
Sverdrup Technology, Brook Park, Ohio 44142

Introduction

IN-FLIGHT, aircraft icing occurs when an aircraft encounters a cloud of small, supercooled water droplets. Therefore, the first step in any complete aircraft icing analysis must include impingement prediction of the water droplets on the critical aircraft surfaces. Traditionally wings have been analyzed using a strip-theory approach and two-dimensional methods. Experimental data on three-dimensional wings have not been available to validate these methods. However, with the recent development of three-dimensional droplet-impingement computational methods,[1-3] the capability now exists to evaluate the accuracy of two-dimensional methods applied to three-dimensional wings. In this technical note a procedure for using two-dimensional droplet-impingement techniques on three-dimensional wings is presented and evaluated against a full three-dimensional code for straight and yawed wings.

Received Feb. 22, 1991; revision received Oct. 15, 1991; accepted for publication Oct. 29, 1991.

*Associate Professor, Department of Aeronautical and Astronautical Engineering. Associate Fellow AIAA.

†Research Engineer, Combustion and Icing Section, LeRC Group. Member AIAA.

Numerical Procedure

Two-Dimensional

Here the Lagrangian, two-dimensional droplet-impingement code of Bragg[4] is used. The trajectory equation given below is a second-order, ordinary differential equation solved by a step-integration scheme:

$$K\left(\frac{d^2x}{d\tau^2}\right) = \frac{C_D R}{24}\left(V - \frac{dx}{d\tau}\right)$$

where K is defined in Table 1, R is the droplet Reynolds number, and C_D is the droplet-drag coefficient. V, x, and τ are the dimensionless local air velocity, droplet-position vector, and time, respectively. K and R_U are often combined[4] into a single dimensionless parameter K_0, the modified inertia parameter, that greatly reduced the analysis. K_0 is given by

$$K_0 = 18K[R_U^{2/3} - (\sqrt{6}/R_U)\arctan(R_U^{1/3}/\sqrt{6})]$$

Several single-droplet trajectories are computed from the freestream, far ahead of the airfoil, until they strike the airfoil. Using this information, a local nondimensional mass flux of droplet-impinging on the surface, referred to as the impingement efficiency, β, can be calculated.

The method for using a two-dimensional analysis to calculate the droplet impingement on a section of a swept or yawed finite wing is summarized in Table 1.

The two-dimensional analysis is performed on an airfoil section perpendicular to the leading-edge where only the component of the freestream velocity, $U_\infty \cos\Lambda$, is seen, therefore, R_U and K are calculated as shown. The two-dimensional analysis is performed at the section-lift coefficient seen by the appropriate section of the three-dimensional wing. In addition, the impingement efficiency β must be reduced by $\cos\Lambda$ since the two-dimensional section is exposed to only that portion of the freestream water droplet concentration.

Three-Dimensional

The three-dimensional droplet impingement code of Mohler[3] is used for comparison to the two-dimensional results. This code uses a three-dimensional surface panel method to generate the three-dimensional flowfield. To save computer time, flowfield velocities are stored at the nodes of a three-dimensional grid system and interpolated to obtain the velocities required by the differential equation solver. The trajectory equation, and the integration scheme, is basically the same as the two-dimensional case, but is done for all three directions x, y, and z. Whereas, the impingement efficiency is determined as a continuous function in the two-dimensional code; here an average value is determined over each panel of interest. The code iterates until a trajectory strikes a panel at each of the four corner points. Thus, the impingement efficiency is formed by the ratio of the effective particle streamtube cross-sectional area far in front of the body, to the surface panel area.

Table 1 Swept or yawed wing two-dimensional calculations

	3D	Equivalent 2D Values
R_U	$\frac{\rho\delta U_\infty}{\mu}$	$\left(\frac{\rho\delta U_\infty}{\mu}\right)\cos\Lambda$
K	$\frac{\sigma\delta^2 U_\infty}{18c\mu}$	$\left(\frac{\sigma\delta^2 U_\infty}{18c\mu}\right)\cos\Lambda$
β	β_{3D}	$\beta_{2D}\cos\Lambda$